



HAL
open science

Estimation of Reactivity Ratios for Olefin Polymerization Catalysts-On the Importance of Thermodynamics

Niyi Ishola, Timothy Mckenna

► **To cite this version:**

Niyi Ishola, Timothy Mckenna. Estimation of Reactivity Ratios for Olefin Polymerization Catalysts-On the Importance of Thermodynamics. *Macromolecular Reaction Engineering*, inPress, 10.1002/mren.202200053 . hal-04042876

HAL Id: hal-04042876

<https://hal.science/hal-04042876>

Submitted on 23 Mar 2023

HAL is a multi-disciplinary open access archive for the deposit and dissemination of scientific research documents, whether they are published or not. The documents may come from teaching and research institutions in France or abroad, or from public or private research centers.

L'archive ouverte pluridisciplinaire **HAL**, est destinée au dépôt et à la diffusion de documents scientifiques de niveau recherche, publiés ou non, émanant des établissements d'enseignement et de recherche français ou étrangers, des laboratoires publics ou privés.

Estimation of Reactivity Ratios for Olefin Polymerization Catalysts – On the importance of thermodynamics

*Niyi B. Ishola, Timothy F.L. McKenna**

CP2M-UMR 5128, Université de Lyon, Bâtiment CPE-Lyon, 43 Blvd du 11 Novembre 1918,
F-69616 Villeurbanne, France

*timothy.mckenna@univ-lyon1.fr

Abstract

A systematic study of the impact of gas phase composition on the estimation of the reactivity ratios of a Ziegler-Natta catalyst during the gas phase copolymerization of ethylene with 1-butene and 1-hexene has been carried out. The results of the study show that if one uses a realistic equation of state to estimate the co- and anti-solubility effects of multiple species in the gas phase, one can obtain a unique value of the reactivity ratio pair from any number of experiments. However, it was found that using only binary solubility data and ignoring the impact of chemically inert species on solubility will lead to the estimate of composition-dependent reactivity ratio pairs.

1. Introduction

The microstructure of polyolefins is the key to the diversity end-use properties and to the success of polyolefins as a choice for many modern materials. It is well accepted polymer microstructure (here meaning the molecular weight and copolymer composition distributions - MWD, CCD - and comonomer sequence length distribution, CSLD) made using coordination catalysts is determined by the temperature and by the concentrations of active species at the catalytic sites. Very commonly, one controls the density of linear low-density polyethylene (LLDPE; a copolymer of ethylene and an alkene such as 1-butene or 1-hexene) by carefully controlling the amount of comonomer incorporated in the polymer chain. The quantity of alkene, as well as the distribution of alkenes along the chain contribute greatly to defining the final physical properties of LLDPE. Very often kinetic models are used in conjunction with reactor models of varying degrees of detail to predict the influence of process conditions on the polymer composition, to control the process and so forth. In the case of copolymerization, the reactivity ratios are important kinetic parameters because they provide important information about copolymer microstructural indicators. While the concept of reactivity ratios was originally developed for free radical polymerization, it is also

a convenient means of describing the tendency of a catalytic site to insert a molecule between the active site and a growing polymer chain as a function of the nature of the last monomer unit in the chain that is attached to said site.

For a system of one monomer (M) and one comonomer (C) these ratios are defined as:

$$r_M = \frac{k_{pMM}}{k_{pMC}} \quad (1)$$

$$r_C = \frac{k_{pCC}}{k_{pCM}} \quad (2)$$

where k_{pMM} and k_{pCC} are the homopolymerization rate constants for monomer and comonomer respectively (i.e. they represent the tendency of a molecule to insert itself between the active site and a chain beginning with same type of molecule), and k_{pMC} and k_{pCM} are the cross propagation constants (i.e. the tendency of a molecule to insert itself between the site and a chain ending in the other type of molecule). Thus, if a reactivity ratio is greater than one, the active site “prefers” to homopolymerize the species in question, otherwise, it prefers inserting the opposite molecule into the chain.

There are different ways of estimating these parameters, but a survey of the literature shows that the most common ways are based on using the Mayo-Lewis equation [1] which is given by:

$$F_M = \frac{r_M f_M^2 + f_M f_C}{r_M f_M^2 + 2f_M f_C + r_C f_C^2} \quad (3)$$

where F_M is the mole fraction of ethylene (assuming ethylene is the principal monomer) in the copolymer, and f_M and f_C are the fractions of monomer and comonomer at the active sites. These last parameters are defined as:

$$f_E = \frac{[E]}{[E]+[C]}, f_C = 1 - f_E \quad (4a, 4b)$$

where [E] and [C] are the concentrations of ethylene and comonomer at the active sites. In the rest of this work, the comonomers are either 1-butene (B), or 1-hexene (H). In the specific case of interest here, this means the concentration of monomer and comonomer in the amorphous phase of the polymer just above the active sites. If one knows these concentrations, ^{13}C NMR can be used to estimate the composition of the polymer, and if the polymer is produced in conditions with no composition drift, equation (3) can be used to fit

the data and obtain the true reactivity ratios. There are of course other methods, such as the Fineman-Ross [1] or Kelen-Tudos [2] methods, that take slightly different approaches, but that also rely on values of the copolymer composition, and the fractions of monomer at the active sites. In other words, regardless of how one estimates the true reactivity ratios, the reliability of the values will depend greatly on the precision of the NMR measures and on the accuracy of the estimation of the monomer and comonomer fractions at the active sites.

Knowing the composition of the monomers at the active sites might be less problematic in a solution polymerization, but in the case of supported catalysts the accumulation of polymer between the bulk phase of the reactor and the sites themselves can make the sorption of the reactive species difficult to calculate. In fact, when two or more species are present in the reactor, cosorption effects can influence the solubility of each of the species in question. The sorption of one or more penetrants in the amorphous phase of semicrystalline polyethylene provokes a change in the free volume of the amorphous polymer, which in turn leads to changes in penetrant solubility and diffusivity[3,4,5].

This means that the solubility of a mixture of penetrants in amorphous PE is different from the sum of the individual solubilities of these penetrants, and the solubility of a single species in the presence of others is different from the solubility of the same species when it dissolves in the polymer as a pure component. For instance, Novak et al. [6] demonstrated very clearly that ethylene is more soluble in LLDPE in the presence of 1-hexene than it is when present as a pure component at the same temperature (T) and pressure (P). Conversely the same authors also showed that the solubility of 1-hexene decreased in the same polymer when ethylene is added to the gas phase. Furthermore, the composition of the gas phase for LLDPE production always contains more than 2 species. Hydrogen is used to control the molecular weight distribution, and chemically inert alkanes are often used in gas phase processes to enhance temperature control [7]. Several studies have demonstrated the importance of these co- and antisolubility effects.[6, 8,9,10,11,12,13], including on both the rate of polymerization [3], and on the physical properties of the copolymers.[14] For instance, Ishola et al.[14] showed that adding a chemically inert compound like pentane to the copolymerization of ethylene and 1-butene leads to a higher crystallinity in the final polymer than one finds for a simple mixture of the same two reactive species.

This signifies that kinetic parameters estimated using simplifying assumptions that the ratio of the monomer and comonomers in the continuous phase of an experiment is the same as at the active site, [15,16,17,18,19,20,21,22,23] or assuming the solubility of individual species in a mixture is simply the sum of the pure component solubilities [24,25,26,27] will

contain biases due to the aforementioned thermodynamic effects. In other words, one could find cases where the reactivity ratios appear to be a function of the composition of the species in the reactor even though this is physically unrealistic. Prediction of the solubility of the reactive species should therefore be done with an equation of state since this approach allows one to account for thermodynamic interactions between the penetrating species and the polymer. While Henry's law can be used to predict the solubility of light components such as methane, ethane, and ethylene over a range of T moderate P, it fails at high pressures of light components, and for heavier components such as alkanes and alkenes. [11,28,29] It is therefore preferred to use an equation of state when trying to predict the solubilities of gas mixtures. The Sanchez-Lacombe (SL-EOS) [30,31] and perturbed-chain statistical associating fluid theory (PC-SAFT) [32] are widely used in for polyolefins, and the advantages of the two approaches have been discussed elsewhere [33]. In the current work we will apply the SL-EOS to calculate the concentration of one, two, or three penetrants in the amorphous phase of PE based on its (relative) simplicity and predictive capability.

SL-EOS treats the polymer chain as a set of beads which are in networked to each other on a lattice. Like a Flory-Huggins model, the polymer chain is assumed to be randomly mixed with penetrant molecules (and thus assumed to be completely amorphous). However, unlike Flory-Huggins model, SL-EOS allows vacant sites in the lattice structure of the polymer to permit change of volume when penetrants and polymer molecules are mixed [31,34] It is important to underline the fact that both the SL-EOS and the PC-SAFT equations of state require semi-empirical interaction parameters that depend on both the composition of the penetrating vapour mixture and the nature of the polymer. Since they were both developed for purely amorphous polymers, but are applied to semi-crystalline systems, the structure of the macromolecular chains can also have an impact on the values of the interaction parameters, so care must be taken to measure their values on polymers like the ones to which one will apply the thermodynamic model.

With these points in mind, the objective of the current paper is to demonstrate that it is still possible to get a set of reactivity ratios that describe the incorporation of a comonomer under a wide range of circumstances when the thermodynamics of sorption deviate from ideal solution thermodynamics by using an equation of state with the right interaction parameters. It will also be shown that using pure component solubilities in a multicomponent system leads to erroneous estimates of the reactivity ratios. To do this for some realistic gas phase compositions, it is also necessary to have a set of interaction parameters for the different mixtures. We will therefore use the pressure decay method developed by M'Rad et al. [9] to

measure the solubilities of the different mixtures and use the data to fit the interaction parameters of the SL-EOS.

In the current paper we will focus on the estimation of the reactivity ratio of ethylene (C2) and 1-hexene (1-C6) and of C2 and 1-butene (1-C4) in different systems in a gas phase polymerization on a supported Ziegler-Natta catalyst. We will demonstrate that it is imperative to account for the composition of the gas phase, and in particular the impact of the presence of chemically inert alkanes when estimating the reactivity ratios.

2. Materials and Methods

2.1 Materials

Argon, hydrogen, ethylene (C2), propane (C3), 1-butene (1-C4), isobutane (iC4) all with a minimum purity of 99.5%, were procured from Air Liquide (Paris, France). Purification columns of zeolite and active carbon were used to purify ethylene before being used. 1-hexene (1-C6) and n-pentane (nC5) with a minimum purity of 99%, was obtained from Sigma-Aldrich ICN (Germany) and was purified through distillation over CaH₂. The co-catalyst (Triethylaluminium) was obtained from Witco (Germany). Two commercial Ziegler-Natta catalysts were used during this work, catalyst 1 was used for the C2 – 1-C6 copolymerization and the C2 – 1-C4 copolymerizations, with and without iC4. Catalyst 2 was used for the other runs.

2.2 Solubility Measurements

The sorption experiments for single and multicomponent vapour mixtures were carried out using the pressure decay method and apparatus described by Ben M'Rad et al. [9], as was the procedure for identifying the interaction parameters for the SL-EOS. The different vapour mixtures considered in this work, as well as the temperatures, pressure ranges and compositions are given in Table S1. The results of the solubility measurements are shown in the Supplemental Information, Figures S2-S5.

2.3 Polymerization procedure

Polymerizations were conducted in a spherical stirred bed semi-batch reactor, using an NaCl bed (40 g) according to the procedure outlined in reference [3]. All polymerization experiments were performed at constant temperature of 70 °C, a constant hydrogen pressure of 1 bar and a time of 15 minutes to keep the conversion of 1-hexene or 1-butene below 10%. At the completion of the reaction, the reactor was depressurized and cooled to room

temperature. The product was collected and washed by water and then dried under vacuum at 70 °C. For the copolymerization involving ethylene/1-hexene, 12 LLDPE copolymers of polyethylene-co-1-hexene were made by varying ethylene (4, 7, 9 bars) and 1-hexene pressure (0.2, 0.4, 0.6, and 0.8 bars) in the absence of any induced condensing agents (ICA). The C2/1-C4 copolymerizations were performed with and without isobutane as ICA. 12 LLDPE copolymers were made at constant ethylene and isobutane pressure of 7 and 3 bar, respectively, while 1-butene pressure was varied from 0.6 – 2.1 bar. For the copolymerization involving ethylene/1-butene in the presence of propane or n-pentane, the reaction condition includes constant pressure of propane (5 bar) or n-pentane (1 bar) and varying ethylene pressure (4 and 7 bar) and 1-butene pressure (0.6 – 1.8 bar). The polymerization rates of these experiments are present in the Supplemental Information, Figure S6-S10.

2.4 Copolymer characterization

Each of the polymer samples was dissolved in a mixture of benzene-d₆/tetrachloroethylene (C₆D₆/TCE) with volume ratio of 2:1 under heating with concentration of 80 mg/mL in a 10 mm tube. Bruker AVANCE II spectrometer operating at 400 MHz for ¹³C and for ¹H at 90 °C. ¹H spectra were recorded under the following operating conditions: zg30 sequence, an acquisition time of 4.09 s, a relaxation delay of 3 s, and 256 scans. ¹³C spectra were recorded under the following operating conditions: zgig70 sequence, an acquisition time of 1.36 s, a relaxation delay of 10 s, and 4000 scans. Residual protons (δ 7.15 ppm) of benzene and backbone carbon Sδ+δ+ (δ 29.58 ppm) of polyethylene were used as an internal reference for ¹H and ¹³C NMR spectra, respectively. The method of Randall [35] was adopted to calculate the copolymer compositions.

2.5 Calculations

Estimation of reactivity ratios

As mentioned above, the reactivity ratio can be estimated from the Mayo-Lewis equation which relates the mole fraction of ethylene in the copolymer (F_E) to ethylene mole fraction in the amorphous phase (f_E) of the polymer. A Levenberg-Marquardt nonlinear least squares algorithm will be used to fit monomer composition obtained from SL-EOS and copolymer composition obtained from ¹³C NMR to Mayo-Lewis equation. This approach takes into account the non-linearity of the Mayo-Lewis equation, and is preferred to using the Fineman-Ross method which is based on linearizing the kinetic model.

Sanchez Lacombe Equation of State

The following terms will be used to describe the different systems under consideration:

- binary refers to a system with one polymer and one penetrant. This is slightly different from a “pure component” system. In a pure component system, we will calculate the binary solubilities of the species present in the vapour phase and assume that the other species present do not influence the solubility;
- ternary refers 2 penetrants and one polymer where we account for the interaction parameters;
- quaternary refers to 3 penetrants and 1 polymer where we account for the interaction parameters.

The mole fractions of the monomer and comonomer in the amorphous polymer were calculated using the SL-EOS for binary [9,30], ternary [31] and quaternary [36] systems. The SL-EOS also requires characteristic parameters for the species of interest. These are known *à priori* and are given in Table S2.

3 Results and discussion

3.1 Solubility Data

The interaction parameters found from the solubility experiments shown in the supplemental material and used in the current work are given in

Table 1. Except for the ethylene co-1-hexene polymerization systems, all of the interaction parameters were found by fitting the data shown in the Supplementary Material. It is not unexpected that the value of k_{12} for the ethylene co-1-hexene system be different from the other binary data as the polymer is not the same as these values were taken from the literature. For this reason, we decided use both the binary and ternary data estimated in reference [38] so that it would be coherent. We will treat this case separately from the others. As we will see below this does not change the conclusions on the role of solubility in estimating the reactivity ratios.

Table 1. Interaction parameters at 70°C for the different polymerizations in the current work.

System	Species (subscript no.)*	k_{ij}	Reference
C2 + 1-C6 + LLDPE	C2 (1)	$k_{12} = 0.038$	[37]
	1-C6 (1)	$k_{12} = 0.027$	[38]
	C2(1) + 1-C6 (2)	$k_{13} = 0.038$ $k_{23} = 0.045$	[38]
C2 + 1-C4 + LLDPE	C2 (1)	$k_{12} = -0.01796$	This work**
	1-C4 (1)	$k_{12} = -0.0019$	This work
	C2 (1) + 1-C4 (2)	$k_{13} = -0.1401$ $k_{23} = 0.0508$	This work
C2+ C3+ 1-C4 + LLDPE	C2 (1) + C3 (2) + 1-C4 (3)	$k_{14} = -0.1414$ $k_{24} = -0.0034$ $k_{34} = 0.0484$	This work
C2+ iC4+ 1-C4 + LLDPE	C2 (1) + iC4(2) + 1-C4 (3)	$k_{14} = -0.0959$ $k_{24} = 0.0443$ $k_{34} = 0.0663$	This work
C2+ nC5+ 1-C4 + LLDPE	nC5 (1)	$k_{12} = 0.0171$	This work
	C2 (1) + nC5 (2) + 1-C4 (3)	$k_{14} = -0.3719$ $k_{24} = 0.1595$ $k_{34} = -0.1128$	This work

*The number of the polymer in the system is always one more than the last penetrant. Number increases from lightest to heaviest component.

** see supplementary material for experimental data

The interaction parameters between the penetrant molecules in the mixture are taken as being equal to zero. In other words, it is assumed that mixtures of ethylene comonomer and ICA behave as ideal mixtures conforming to Lorentz-Berthelot combining rules.[39]

3.2 Reactivity Ratios

3.2.1 Two component mixtures: polyethylene-co-1-hexene

12 LLDPE copolymers of polyethylene-co-1-hexene were made by varying ethylene (4, 7, 9bar) and 1-hexene pressure (0.2 –0.8 bar). The different copolymer composition distributions measured using ^{13}C NMR are given in

Table 2. Note that in this table the meaning of the names of each run is as follows: E_xH_y refers to a run with ethylene (E) and 1-hexene (H) where the ethylene pressure in the gas phase is x bars and that of 1-hexene y bars. In this Table, the terms binary and ternary refer to the definitions given above. In other words, $f_E(\text{binary})$ refers to a copolymer composition calculated using pure component solubilities, and $f_E(\text{ternary})$ refers to a copolymer composition calculated using ternary solubilities (i.e. that take into consideration the cosolubility effect).

Table 2. Copolymer composition, monomer fraction at the active sites using binary and ternary SL-EOS

Run	F_E (^{13}C NMR)	f_E (binary)	f_E (ternary)
$E_4H_{0.2}$	0.98	0.16	0.18
$E_4H_{0.4}$	0.95	0.084	0.11
$E_4H_{0.6}$	0.93	0.054	0.076
$E_4H_{0.8}$	0.91	0.038	0.061
$E_7H_{0.2}$	0.99	0.25	0.29
$E_7H_{0.4}$	0.98	0.14	0.17
$E_7H_{0.6}$	0.97	0.09	0.12
$E_7H_{0.8}$	0.96	0.064	0.098
$E_9H_{0.2}$	0.99	0.30	0.35
$E_9H_{0.4}$	0.99	0.17	0.21
$E_9H_{0.6}$	0.98	0.11	0.15
$E_9H_{0.8}$	0.96	0.081	0.12

The estimation of the reactivity ratios was done using Levenberg-Marquardt nonlinear least squares algorithm by fitting an experimental data set to the Mayo-Lewis equation (Equation 3). The estimates were obtained by minimizing the sum of squares of the residuals between model predictions and experimental data. The reactivity ratios estimated using binary and ternary solubilities are given in Table 3 along with the values of the confidence interval as well as the sum of squares of the residuals. It can be seen from Figure 1 that the joint

confidence region for the values calculated from the binary solubility data includes a value of 0 for r_H , indicating that this value is statistically insignificant. The data fit is slightly better when the ternary data are used (R^2 is slightly higher), and that the values from both reactivity ratios are statistically significant at 95% confidence when the ternary solubility data is used. Nevertheless, it can be seen from the Mayo-Lewis plots in Figure 2 that the estimates of copolymer composition obtained using both binary solubilities and ternary solubilities are acceptable for all practical purposes if one needs to calculate copolymer compositions over the range of pressures studied. However, as we shall see below one cannot generalize this conclusion to all systems of interest. In the case of the ethylene co-1-hexene polymerizations presented in this section, only 2 gas phase components have been considered. However, it is more common to find several penetrants in a commercial scale plant, especially if one is running a gas phase polymerization in condensed mode where one can find one or more alkanes in the reactor in addition to monomer and comonomers. For this reason, this same analysis will be extended to multicomponent systems in the next section.

Table 3. Reactivity ratios for Ethylene/1-hexene copolymerization and the JCR result.

Parameter	Binary system			Ternary system		
	values	Confidence interval		values	Confidence interval	
		lower	higher		lower	higher
r_E	293	198	387	265.16	182.72	347.59
r_H	0.009	-0.01	0.03	0.05	0.009	0.092
R^2	0.9392			0.9719		

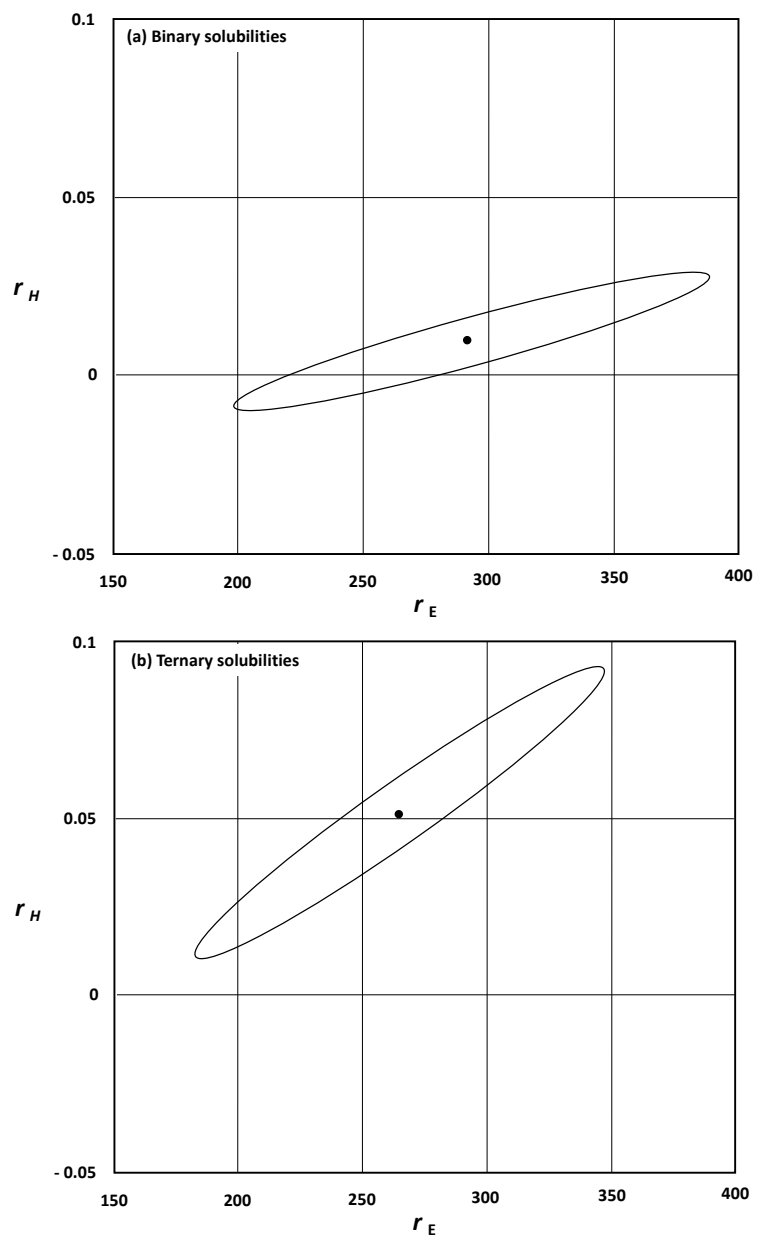


Figure 1. Plot of 95% joint confidence region for ethylene/1-hexene copolymerization; (a) binary and (b) ternary systems.

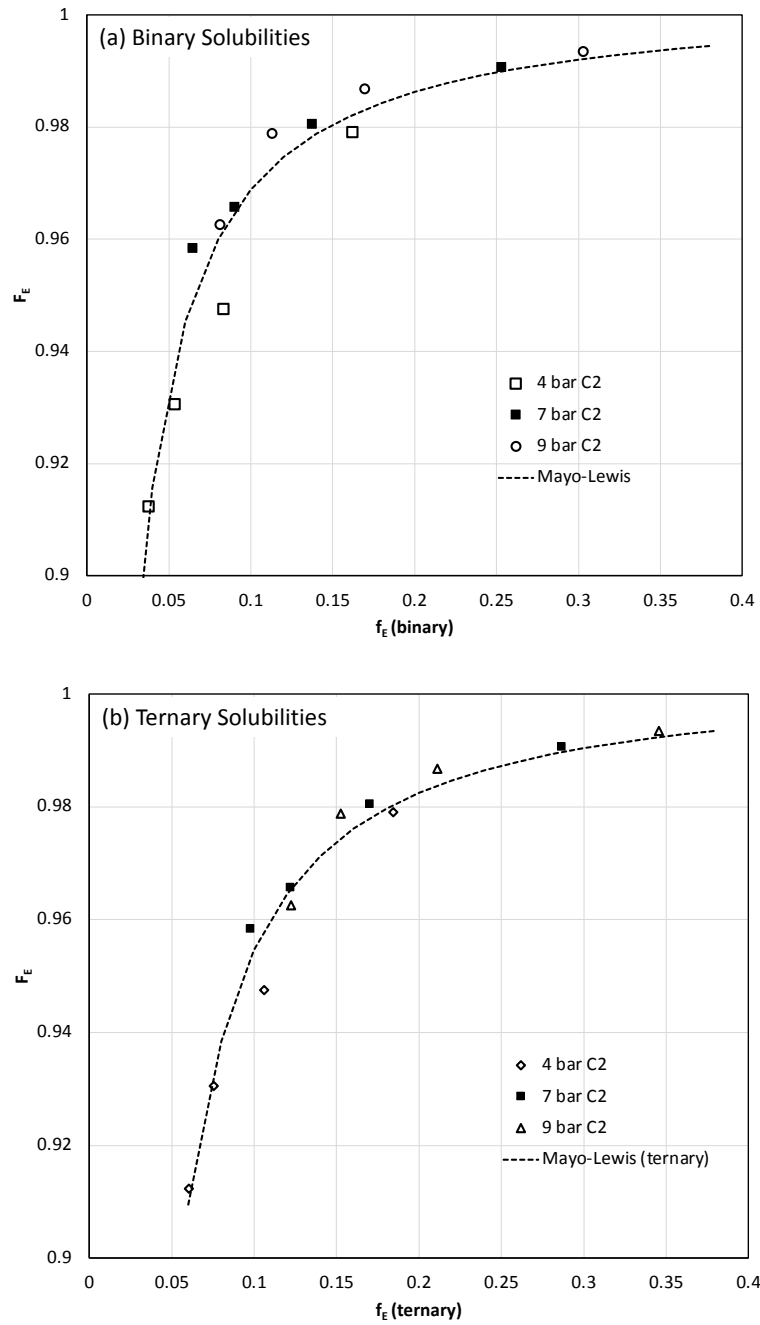


Figure 2. Copolymer composition versus monomer composition in amorphous fraction of the polymer of (a) binary and (b) ternary solubility calculations for ethylene/1-hexene copolymers.

The difference between the two cases (binary vs ternary solubilities) shown in this example shows that it is preferential to consider a more accurate thermodynamic model, but for all intents and purposes, the difference between the two is not significant. The reason for this is

while there is a cosolubility effect of hexene on ethylene, Figure 3 shows that this is not particularly pronounced. However, if the gas phase composition leads to more significant cosolubility effects, the choice of thermodynamic model can become important.

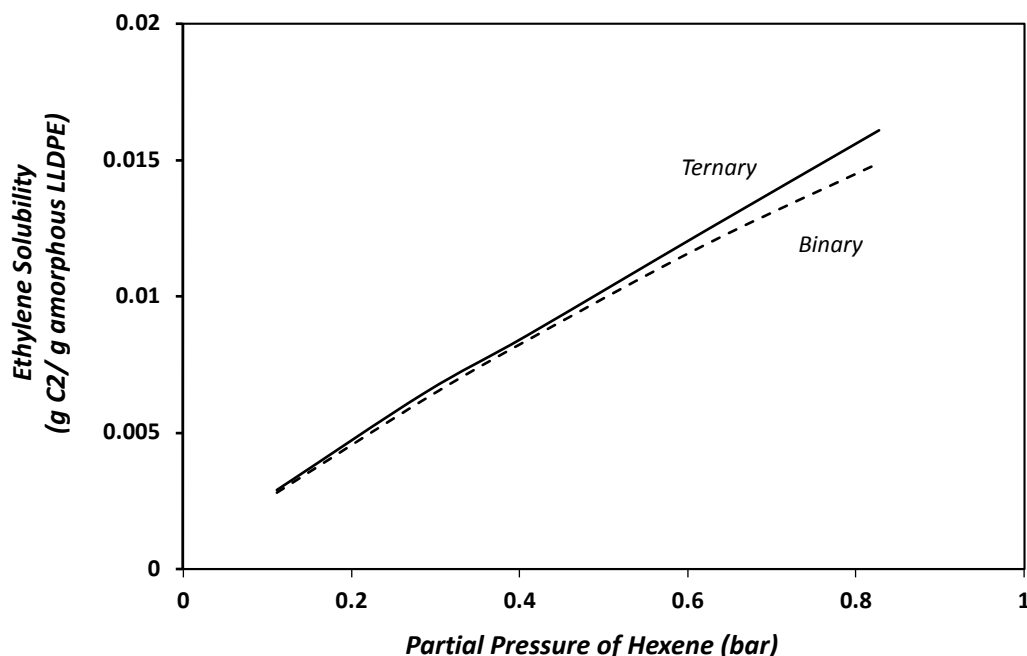


Figure 3. Cosolubility effect of hexene on ethylene (7 bars ethylene, 70°C) represented by the Ternary model. The Binary example does not account for the cosolubility.

3.2.2 Multicomponent mixtures: ethylene co-1-butene + alkanes

In this section, we will evaluate the reactivity ratios for ethylene co-1-butene in the case of 2 and different 3 component gas mixtures. As one can see from the results in section S2.3 of the Supplementary material, the solubility of ethylene in the amorphous phase of LLDPE can vary over a wide range when an alkane is present in addition to the comonomer. The copolymer composition for the different runs is shown in Table 4 and the ethylene mol fraction in the amorphous phase of the polymer is given in Table 5 using different methods of calculation. In this last table, Ternary refers to the ternary SL-EOS in the absence of any induced condensing agent (no alkane) that accounts for the cosolubility effects between ethylene and 1-butene. The quaternary models include the alkane in addition to the other gaseous species.

Table 4. Copolymer compositions for the different multicomponent mixtures during the polymerization of ethylene co-1-butene.

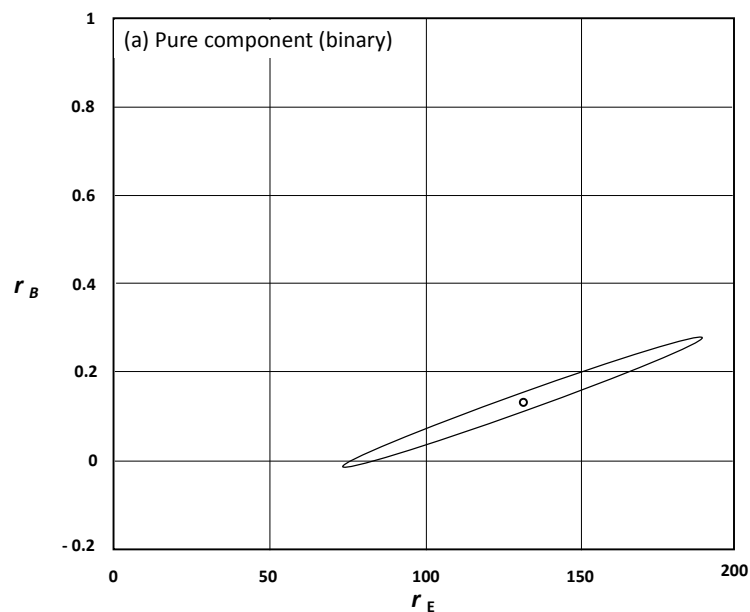
Run	Copolymer Composition (F_E) - NMR			
	0 alkane	3 bar iC4	5 bar C3	1 bar nC5
E ₄ B _{0.6}	0.97	-	0.97	0.98
E ₄ B _{0.9}	0.93	-	0.95	0.96
E ₄ B _{1.2}	0.92	-	0.94	0.93
E ₄ B _{1.5}	0.91	-	0.92	0.92
E ₄ B _{1.8}	0.86	-	0.89	0.89
E ₇ B _{0.6}	0.99	0.99	0.98	0.99
E ₇ B _{0.9}	0.98	0.98	0.98	0.98
E ₇ B _{1.2}	0.96	0.97	0.96	0.97
E ₇ B _{1.5}	0.95	0.96	0.96	0.97
E ₇ B _{1.8}	0.94	0.94	0.95	0.96
E ₇ B _{2.1}	0.93	0.93	-	-

Table 5. Ethylene mol fraction in the amorphous phase of the polymer the different multicomponent mixtures during the polymerization of ethylene co-1-butene predicted using different thermodynamic models.

Run	Ethylene Fraction in Amorphous Polymer (f_E)				
	Pure Component (binary)	Ternary (no alkane)	Quaternary 3 bar iC4	Quaternary 5 bar C3	Quaternary 1 bar nC5
E ₄ B _{0.6}	0.26	0.75	-	0.79	0.82
E ₄ B _{0.9}	0.19	0.67	-	0.70	0.69
E ₄ B _{1.2}	0.15	0.61	-	0.63	0.60
E ₄ B _{1.5}	0.12	0.58	-	0.58	0.53
E ₄ B _{1.8}	0.10	0.50	-	0.53	0.48
E ₇ B _{0.6}	0.38	0.89	0.91	0.87	0.91
E ₇ B _{0.9}	0.29	0.80	0.84	0.81	0.83
E ₇ B _{1.2}	0.23	0.73	0.77	0.75	0.76
E ₇ B _{1.5}	0.19	0.66	0.72	0.72	0.71
E ₇ B _{1.8}	0.16	0.64	0.67	0.70	0.70
E ₇ B _{2.1}	0.15	0.60	0.62	-	-

Let us first consider the estimation of the reactivity ratio the ethylene co-1-butene polymerization in the presence of isobutane as ICA at an ethylene pressure of 7 bars

(experiments E₇B_{0.6} - E₇B_{2.1}). The estimated reactivity ratios for copolymerizations at 7 bars of ethylene, the upper and lower bounds of the 95% confidence intervals, and the coefficient of determination (R^2) are given in Table 6. If we compare reactivity ratios based on pure component solubility (binary) with those estimated using ethylene mol fractions calculated using a SL-EOS that accounts for penetrant mixture composition, two main observations can be made. First, if one does not account for the thermodynamic interactions of the penetrating species (i.e., one uses pure component or binary solubility models), then predicted pair of reactivity ratios is 131 for C₂ and 0.13 for butene. Furthermore, the latter is not statistically different from zero with this limited data set. These values are very different from those in the second column (Ternary Solubility), where the reactivity ratios for ethylene and for butene are both statistically significant, and quite different from the binary values. The second important observation is that when one uses the correct thermodynamic representation, the estimated reactivity ratios are very close for the cases where one does and does not include iC₄ as an ICA. This is important since it means that even if we change the mixture composition, and thus the ethylene concentration in the amorphous phase (see Table 5), we will find essentially the same values for the reactivity ratio. It can be seen from the graphs in Figure 4 that the JCR found with thermodynamic models that account for the solubility effect are very close. Ideally, they would overlap of course, but with the limited data sets it was possible to generate, such small differences do not appear to be important with respect to the values calculated using the pure component solubilities.



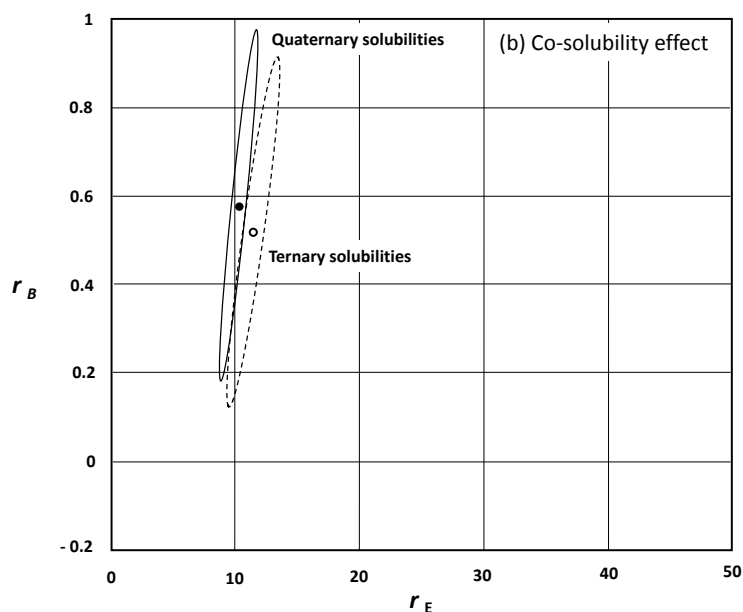


Figure 4. Plot of 95% joint confidence region for ethylene/1-butene copolymerization in the presence of isobutane as ICA for (a) pure component solubility and (b) accounting for the cosolubility effect. 7 bars of ethylene, 1 bar 1-C4, 0 and 3 bars of iC4.

Table 6. Reactivity ratios and Joint Confidence Region for Ethylene co-1-butene polymerization at 7 bars of ethylene, with and without isobutane.

	Binary Solubility		Ternary Solubility (no iC4)		Quaternary Solubility (3 bars iC4)				
	95% JCR		95% JCR		95% JCR				
	Lower	Upper	Lower	Upper	Lower	Upper			
r_E	131	74	188	11.4	9.4	13.3	10	8.8	11.9
r_B	0.13	-0.01	0.28	0.52	0.14	0.89	0.58	0.21	0.95
R^2	0.9891		0.9975		0.9980				

If we enlarge the data set to include 4 and 7 bars of ethylene, it can be seen from Table 7 that the reactivity ratios calculated using binary (pure component) solubilities are different from those in Table 6. In other words, changing the compositions of the mixtures changes the reactivity ratios – which clearly it should not! On the other hand if thermodynamic interactions are accounted for (Ternary Solubility), then we find a value of the reactivity ratio pair this is very close to that of those shown in Table 6. Finally, repeating this analysis for ethylene co-1-butene polymerizations in the presence of 5 bars of propane or 1 bar of n-pentane and accounting for the interactions of the penetrant species (c.f. Table 8, Quaternary

Solubility), leads once again to reactivity ratios that are very close to those shown in the previous two Tables.

Table 7. Reactivity ratios and Joint Confidence Region for Ethylene co-1-butene polymerization at 4 and 7 bars of ethylene

	Binary Solubility		Ternary Solubility (no alkane)			
	95% JCR		95% JCR			
	Lower	Upper	Lower	Upper		
r_E	75	54	96	9.2	7.7	10.8
r_B	0.04	-0.01	0.09	0.62	0.30	0.98
R^2	0.9825			0.9905		

Table 8. Reactivity ratios and Joint Confidence Region for Ethylene co-1-butene polymerization at 4 and 7 bars of ethylene for C3 and nC5 alkanes.

	Quaternary Solubility (5 bar C3)		Quaternary Solubility (1 bars C3)			
	95% JCR		95% JCR			
	Lower	Upper	Lower	Upper		
r_E	10.7	8.5	13	11.4	9.3	13
r_B	0.6	0.15	0.98	0.32	0.06	0.57
R^2	0.9839			0.9884		

The reason for the importance of correctly accounting for the cosolubility effects when estimating the reactivity ratios can be seen in Figure 5 for the system C2/1-C4/C3. It can be seen here that the compositions of ethylene and of butene in the amorphous polymer with no propane are quite different from those estimated as one adds propane to the gas phase mixture. In this particular instance, propane acts as a cosolvent for ethylene, enhancing the solubility of the latter in the amorphous phase of the polymer, and as an anti-solvent for 1-butene. Further examination of Figure 5 also shows that while there is an antisolvent effect, it is weak and the main contribution to the change in local monomer concentration will be the cosolubility effect. The impact of this effect increases as the pressure of propane increases. One can observe similar effects for the other systems considered here. This demonstrates that relative amounts of ethylene and of 1-butene at the active sites will be a function of the

concentration of inert species in the gas phase mixtures, and if one did not account for this when estimating the reactivity ratios (and other kinetic constants!), then the values of the reactivity ratios could in fact appear to be a function of the concentration of inter species in the reactor, which is nonsense.

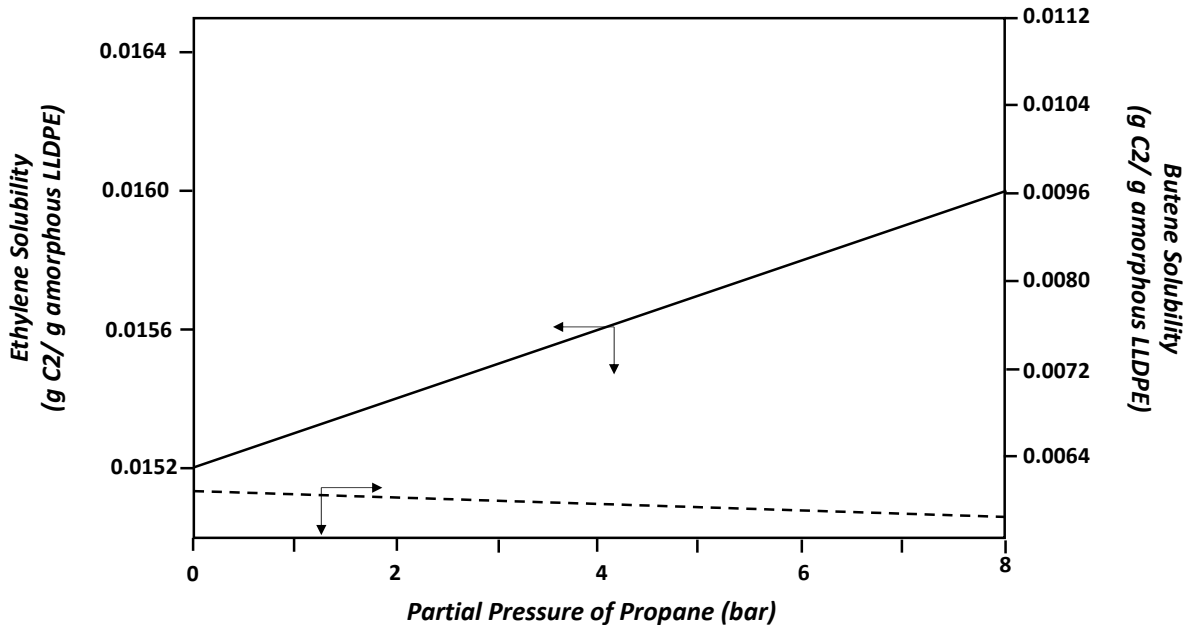


Figure 5. Example of the cosolubility effect of propane on a mixture of 7 bars of ethylene and 1 bar of 1-butene at 70°C.

To summarize the importance of this approach, one can consider the plot in Figure 6. This graph shows two Mayo-Lewis plots: one using an average value of the “correct” reactivity ratios estimated using the SL-EOS from Tables 6-8 ($r_E=10.5$ and $r_B=0.53$), and one using the reactivity ratios using the binary calculations shown in Table 7. Clearly, the use of a thermodynamic approach that allows for co- and antisolubility effects allows us to the reactivity ratios calculated from one data set to successfully model any other data set (provided we always use the same thermodynamic approach). On the other had, the use of reactivity ratios that fit a given data set, but that are calculated with binary reactivity ratios is not reliable at all.

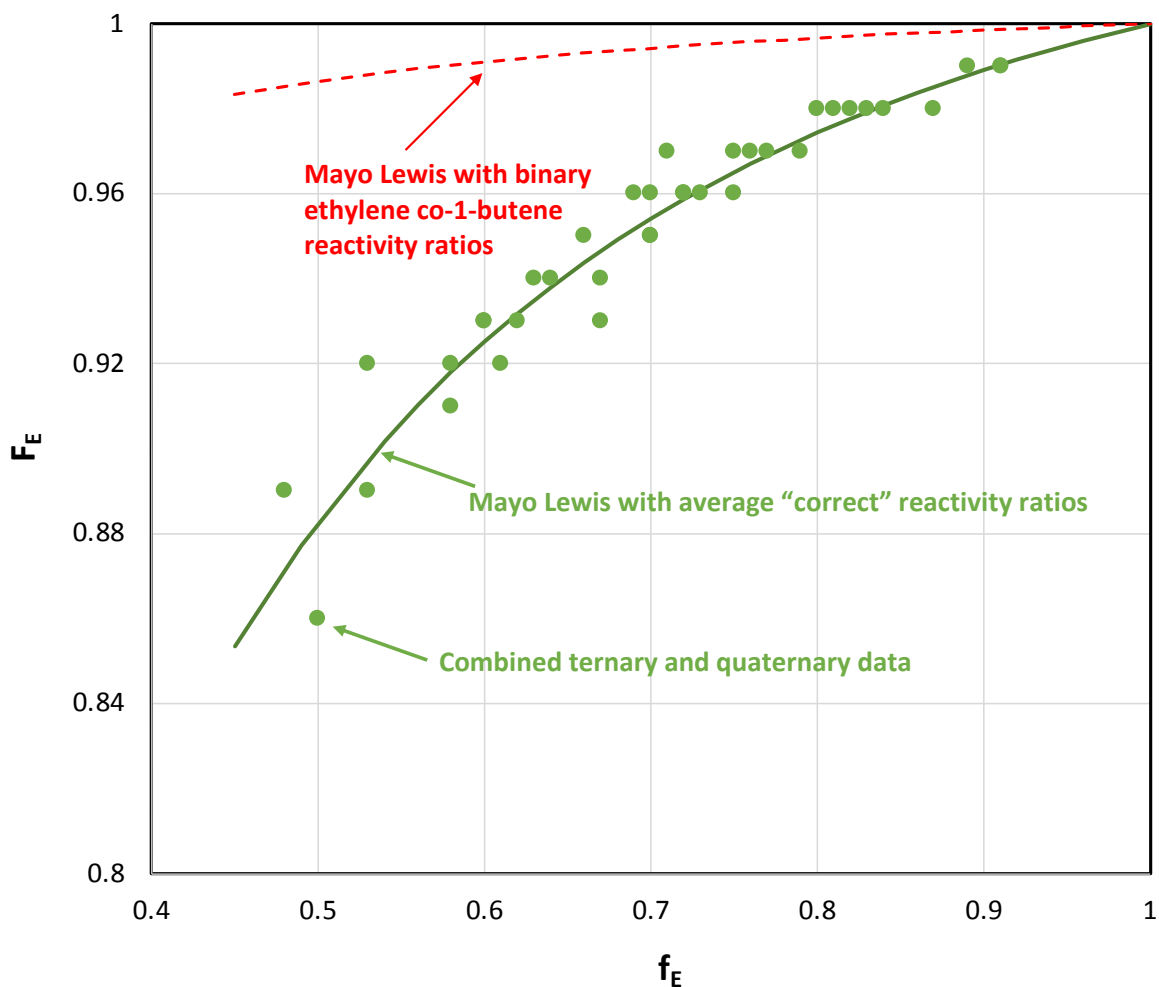


Figure 6. Mayo-Lewis plot for the ensemble of ternary and quaternary data from Tables 6-8 (data points), with an average value of the reactivity ratios estimated using the SL-EOS accounting for interactions ($r_E=10.5$, $r_B=0.53$) and the copolymer compositions calculated using the binary reactivity ratios in Table 7.

4. Conclusion

The importance of accounting for cosolubility effects when estimated the reactivity ratios of gas phase olefin copolymerizations has been demonstrated. In certain simple cases, such as the copolymerization of ethylene and 1-hexene, accounting for the cosolubility effects over a narrow composition range does not appear to be critical. However, if one were to add a typical amount of induced condensing agent to this system (as would be typical in an industrial context), this is no longer true.

In the case of ethylene and 1-butene copolymerizations, the cosolubility effect corresponding to the mixture compositions make it important to consider the thermodynamic model used to

estimate component solubilities for the calculation of reactivity ratios. Furthermore, as the complexity of the mixture increases, it becomes very difficult to ignore co- and anti-solubility effects. It is therefore important to have a good thermodynamic representation of the solubilities of the reactivity species of interest in multicomponent systems.

5. References

1. M. Finemen, S.P. Ross, *J. Poly. Sci.*, **1950**, 5, 259.
2. T. Kelen, K. Tudos, *J. Macromol. Sci.: Part A - Chem.*, **1975**, 9, 1.
3. A. Alizadeh, M. Namkajorn, E. Somsook, T.F.L. McKenna, *Macromol. Chem. Phys.*, **2015**, 216, 903.
4. A. Alizadeh, M. Namkajorn, E. Somsook, T.F.L. McKenna, *Macromol. Chem. Phys.*, **2015**, 216, 985.
5. R.F. Alves, T.F.L. McKenna, *Chem. Eng. J.*, **2020**, 383, 123114.
6. A. Novak, M. Bobak, J. Kosek, B. Banaszak, D. Lo, T. Widya, W.H. Ray, J.J. de Pablo, *J. Appl. Polym. Sci.*, **2006**, 100, 1124.
7. T.F.L. McKenna, *Macromol. Reactn. Engng.*, **2019**, 13, 1800026.
8. A. Ben Mrad, N. Sheibat-Othman, J. Hill, M. Bartke, T.F.L. McKenna, *Chem. Eng. J.*, **2021**, 421, 127778.
9. A. Ben Mrad, N. Sheibat-Othman, S. Norsic, T.F.L. McKenna, *Ind. Eng. Chem. Res.*, **2020**, 60, 10791.
10. W. Yao, X. Hu, Y. Yang, *J. Appl. Polym. Sci.*, 2007, 104, 3654.
11. J.A. Moebus, B.R. Greenhalgh *Macromol. Reactn. Engng.*, **2018**, 12: 1700072
12. B.J. Savatsky, Moebus JA, Greenhalgh BR J.A. Moebus, B.R. Greenhalgh *Macromol. Reactn. Engng.*, 2019, 13:1900003
13. J. Sun, H. Wang, M. Chen, J. Ye, B. Jiang, J. Wang, Y. Yang, C. Ren, *J. Appl. Polym. Sci.*, **2017**, 134 (8)
14. N. Ishola, F.N. Andrade, F. Machado, T.F.L. McKenna, *Macromol. React. Eng.*, **2020**, 2000021.
15. I. Caldera, J.B.P. Soares, P.J. Deslauriers, J.S. Fodor, *J. Catalysis*, **2019**, 375, 140.
16. F.M.B. Coutinho, J.L. Xavier-Luna, *Eur Polym J*, **1997**, 33, 897.
17. K. Czaja, M. Białek, *Polymer* , **2001**, 42, 2289.
18. Y.V. Kissin, D.L. Beach, *J. Polym. Sci., Polym. Chem. Ed.*, **1983**, 21, 1065.
19. C. Cozewith, G. ver Strate, *Macromol.*, **1971**, 4, 482.

20. Z. Zhoa, T.B. Midenas, V.A. Zkharov, M.I. Nikolaeva, M.A. Matsko, E.V. Bessudnove, W.Wu, *Polyolefins J.*, **2019**, *6*, 117.
21. S. Mehdiabadi, O. Lhost, A. Vantomme, J.B.P. Soares, *Macromol. Reactn. Engng.*, **2021**, *15*: 2100041
22. M.A. Al- Saleh, J.B.P. Soares, T.A. Duever, *Macromol. Reactn. Engng.*, **2010**, *4*, 578.
23. M.A. Al- Saleh, J.B.P. Soares, T.A. Duever, *Macromol. Reactn. Engng.*, **2011**, *5*, 587.
24. D.M. Sarzotti, J.B. Soares, A. Penlidis, *J. Polym. Sci., Part B – Polym. Phys.*, **2002**, *40*, 2595.
25. M.F. Bergstra, G. Weickert, G.B. Meier, *Macromol. Reactn. Engng.*, **2009**, *3*, 433.
26. J.S. Yoon, *Eur. Polym. J.*, **1995**, *31*, 999.
27. S. Chakravarti, W.H. Ray, *J. Appl. Polym. Sci.*, **2001**, *80*, 1096.
28. C. Rogers, V. Stannett, M. Szwarc, *J. Phys. Chem.*, **1959**, *63*, 1406.
29. C. Rogers, V. Stannett, M. Szwarc, *J. Polym. Sci.*, **1960**, *45*, 61.
30. I.C. Sanchez, R.H. Lacombe, *J. Polym. Sci. B Polym. Lett. Ed.*, **1977**, *15*, 71.
31. I.C. Sanchez, R.H. Lacombe, *Macromol.*, **1978**, *11*, 1145.
32. J. Gross, G. Sadowski, *Ind. Eng. Chem. Res.*, **2001**, *40*, 1244 **40**.
33. A. Alizadeh, J. Chmelař, F. Sharif, M. Ebrahimi, J. Kosek, T.F.L. McKenna, *Ind. Eng. Chem. Res.*, **2017**, *56*, 1168.
34. R. Hariharan, B. Freeman, R. Carbonell, G. Sarti, *J. Appl. Polym. Sci.*, **1993**, *50*, 1781.
35. J.C. Randall, *J. Macromol. Sci. – Rev. Macromol. Chem. Phys.*, **1989**, *29*, 201
36. A. Bashir, V. Monteil, V. Kanellopoulos, M. Al-Haj Ali, T.F.L. McKenna, *Ind. Eng. Chem. Res.*, **2013**, *52*, 16491.
37. M.A. Bashir, M.A-h. Ali, V. Kanellopoulos, J. Seppälä, *Fluid Phase Eq.*, **2013**, *358*, 83.
38. M. Minelli, M.G. De Angelis, , *Fluid Phase Eq.*, **2014**, *367*, 173.
39. A.S. Michaels, H.J. Bixler, *J. Polym. Sci.*, **1961**, *50*, 393.